Radiology Case Reports 15 (2020) 1250–1255

Available online at www.sciencedirect.com

ScienceDirect

journal homepage: www.elsevier.com/locate/radcr

Case Report

Pre- and postnatal MR imaging of an asymptomatic giant hypothalamic hamartoma ☆

Alberto Cristobal, BS[a,*], *Gregory Vorona, MD*[b], *Ann Ritter, MD*[b], *Susan Lanni, MD*[b], *Jacqueline Urbine, MD*[b]

[a] *Virginia Commonwealth University School of Medicine, 1201 E. Marshall St #4-100, Richmond, VA 23298*
[b] *Virginia Commonwealth University Medical Center, Richmond, VA*

ARTICLE INFO

Article history:
Received 1 May 2020
Revised 18 May 2020
Accepted 19 May 2020

Keywords:
Giant hypothalamic hamartoma
Prenatal
Neonate
MRI

ABSTRACT

Hypothalamic hamartomas are rare tumors that are most often diagnosed in early childhood. These lesions are classified as giant hypothalamic hamartomas when they exceed 4 cm in any 1 dimension. The most common presenting symptoms associated with these lesions are precocious puberty, gelastic seizures, and (less commonly) syndromic conditions such as Pallister-Hall syndrome. We present a unique case of an asymptomatic giant hypothalamic hamartoma diagnosed prenatally by fetal magnetic resonance imaging and followed throughout infancy. This case demonstrates the utility of multimetric analysis using difference sequences, including diffuse-weighted imaging, to assess specific properties of intracranial lesions detected in utero and to aid in accurate diagnosis prior to birth.

Introduction

Hypothalamic hamartomas (HH) are rare, tumor-like masses made of an abnormal mixture of normal neural elements that grow commensurate with the brain [1]. Although different proposed classification systems exist [2–4], there are 2 main described subtypes, parahypothalamic and intrahypothalamic [5]. Parahypothalamic hamartomas typically present as pedunculated masses which extend from the region of the tuber cinereum and which are associated with precocious puberty. Intrahypothalamic hamartomas tend to be sessile masses located more posteriorly, and are associated with epilepsy [1,6].

HH are typically <2 cm in size but rarely these can exceed >4 cm. When these lesions exceed 4 cm in any 1 dimension, they are classified as giant hypothalamic hamartomas (GHH). GHH are often diagnosed even earlier in life than HH due to symptoms of mass effect [7–9]. To the best of our knowledge, only a few cases of GHH imaged prenatally by fetal MR have been published, with the diagnosis of GHH in these cases only definitely made after the patient was born and postnatal imaging or biopsy was performed [5,10,11]. Our case is unique as the correct diagnosis of GHH was made by

☆ Conflicts of Interest: None.

* Corresponding author.
E-mail address: cristobala@vcu.edu (A. Cristobal).

https://doi.org/10.1016/j.radcr.2020.05.041

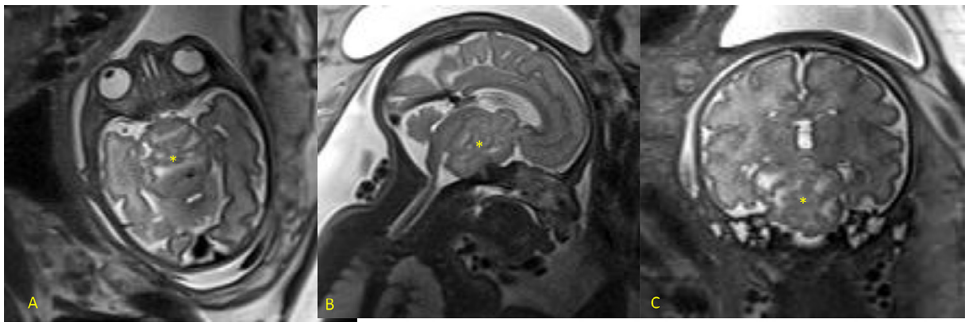

Fig. 1 – Axial (A), sagittal (B), and coronal (D) T2 images of the 35 week fetus demonstrating a large, heterogenous mass (indicated by *) extending from the suprasellar cistern into the prepontine cistern, with posterior displacement and distortion of the brainstem.

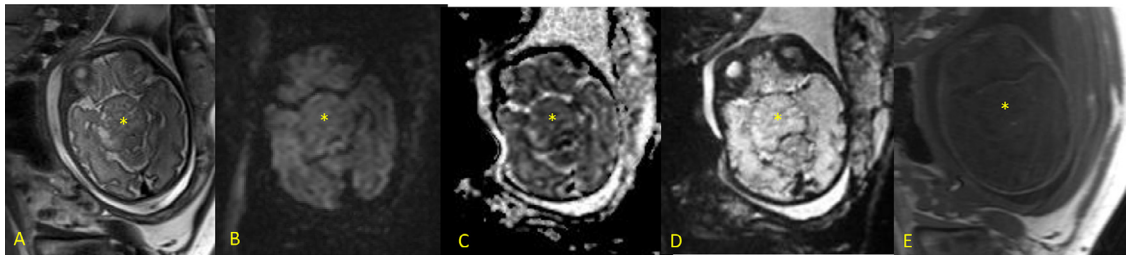

Fig. 2 – Axial T2 (A), DWI (B), ADC (C), echo planar (D), and T1 (E) imaging of the 35 week fetus through the mass (indicated by *). The mass demonstrates similar diffusion characteristics (B and C) relative to the normal brain, without areas of restricted diffusion to demonstrate hypercellularity. No foci of susceptibility artifact (D) or T1 shortening (E) are identified to demonstrate intralesional calcification or hemorrhage.

fetal MRI, and that there has been no prior report of using diffusion-weighted imaging (DWI) in the assessment of GHH during fetal MR.

Case Report

A 30-year-old G2 P0A0L1 female was referred for fetal MRI after an abnormal echogenic mass measuring 2.9 × 3.8 cm within the fetal brain was discovered by ultrasound performed at 32 weeks gestation at an outside institution. Reported internal echogenic components raised suspicion for either an area of hemorrhage or calcifications in the setting of a teratoma. On ultrasound, amniotic fluid was normal, fetal growth was appropriate for gestational age, and head circumference was normal. The patient had declined previous screening for fetal aneuploidies and otherwise had an uneventful pregnancy.

Fetal MRI was performed at 35 weeks gestation on a 3 Tesla MRI scanner utilizing T2 single shot T2, T1 spoiled gradient echo, echo planar, as well as DWI sequences. A 3.9 × 3.6 × 4.1 cm heterogeneous midline mass was identified centered within the suprasellar space. The mass demonstrated signal characteristics approximating normal cortex and white matter on the T2 sequences. There were scattered T2 hyperintense foci within the mass, though no definitive areas of internal cystic change were identified (Fig. 1). No foci of T1 shortening or susceptibility artifact were identified to demonstrate calcification or blood products. The mass demonstrated identical diffusion characteristics compared with the adjacent normal brain parenchyma (Fig. 2). The mass extended superiorly into the inferior aspect of the third ventricle. The mass also extended posteriorly, approximating the ventral midbrain and pons, causing distortion and posterior displacement of the brainstem. The basilar artery was visualized interposed between the mass and the pons. The cerebral aqueduct was patent. A component of the mass extended laterally over the left tentorium into the left middle cranial fossa. Additionally, the mass extended inferiorly into the suprasellar region, with a portion of the mass approximating the clivus. The bilateral internal carotid arteries and proximal aspects of the middle cerebral arteries approximated the anterior aspect of the mass. Given these findings, the leading differential consideration was a giant hypothalamic hamartoma.

A fetal ultrasound was subsequently performed at our institution at 37 weeks gestation, which demonstrated a mass corresponding the findings described above which was mildly hyperechoic relative to the adjacent brain parenchyma (Fig. 3.). The mass was estimated to measure slightly larger in size, at 4.2 × 4.2 × 3.9 cm. No internal hyperechoic foci or areas of internal cystic change were identified.

The mother presented to our institution at 40 weeks 3 days gestation for elective induction of labor. A 3.18 kg baby was delivered vaginally at 40 weeks 4 days gestation vaginally without complication with Apgars of 9 and 9 at 1 and 5 minutes, respectively. The NICU team was present at bedside during de-

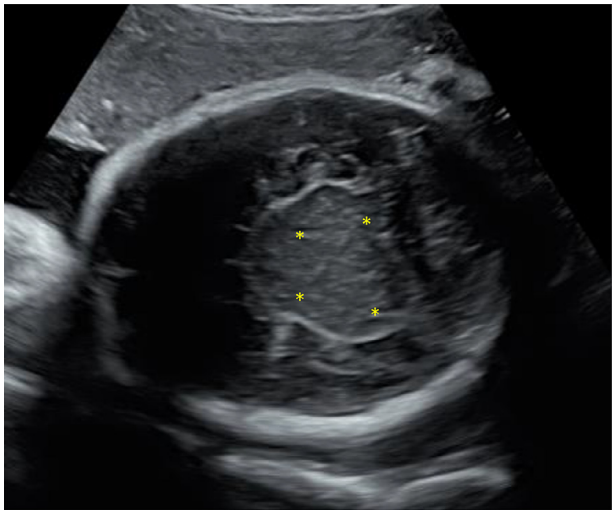

Fig. 3 – Transverse sonograph view of the fetal brain performed at 37 weeks gestation, at the level of the mass (indicated by *). The mass is mildly hyperechoic relative to the surrounding brain parenchyma.

livery due to concern of possible respiratory distress at birth given the evidence of brainstem distortion by the lesion. Fortunately, the infant was well-appearing without physical abnormalities and was admitted to the newborn nursery for routine care.

A postnatal MRI on a 1.5 Tesla scanner was obtained on the same day of delivery which revealed a 5.0 × 3.4 × 3.9 cm mass, indicating that the mass had grown from the prenatal MRI performed approximately 5 weeks prior, but in proportion to the whole brain. The characteristics of the mass were overall unchanged. The leading diagnosis remained a GHH.

Subsequent MR imaging at 3 and 5 months performed on both 1.5 and 3 T MRI units showed continued interval increase in size of the mass commensurate to the growth of the brain (Fig. 4). MRI at 8 months showed stable size of the mass from prior, though it was noted that cystic areas within the mass had small increases in size. At 8 months, a MR spectroscopy study was also performed, with the mass on single-voxel intermediate (TE = 135 ms) spectroscopic imaging demonstrating a diminished N-acetylaspartate relative to the right basal ganglia. Otherwise, the mass demonstrated major metabolic peaks (choline and creatine) similar to normal brain parenchyma (Fig. 5).

To date, the patient has shown normal development. Laboratory evaluation has been unsuggestive of any endocrinologic abnormalities. There was concern of possible seizure-like activity involving lip quivering and 2 leftward head jerks following anesthesia for the 8-month MRI though there had been no similar reports by the parents prior. Follow-up electroencephalogram returned normal and there have been no further episodes since the episode. The patient has been followed closely by the medical genetics, child neurology, and neurosurgical teams at our institution. The patient is 11 months of age at the time of this publication.

Discussion

HHs are congenital, nonneoplastic, tumor-like lesions comprised of heterotopic gray matter, neurons, glial cells, and fiber bundles [10,12,13]. HH are most commonly <2 cm in size with an average reported size of approximately 1.8 cm [7]. Very rarely these lesions exceed 4 cm in which they are then known as GHHs [7,14,15]. The reported incidence of HH is around 1 in 200,000 people. Even fewer are afflicted by GHH [7,14,16]. HH are usually identified in infancy and early childhood (mean age of presentation = 2.5 years) [7] while the majority of GHH are diagnosed within the first few days of life [9]. HH typically come to clinical attention due to central precocious puberty (~60%), gelastic seizures (~60%), or both (~20%) [7,9,11–22]. Less frequently, HH and GHH present later in life with focal neurological changes, signs of increased intracranial pressure [8], or developmental changes [9,14,23].

Interestingly, there is at least 1 reported case in which the temporal sequence was reversed, with the patient initially having atonic and generalized tonic-clonic seizures followed by gelastic seizures that began occurring in early adulthood [22]. This suggests that some patients with seizure disorders of unknown etiology could possibly have undiagnosed HH.

There have been a limited number of cases of GHH that have been published in literature [7–9,14–16,20–25] and only

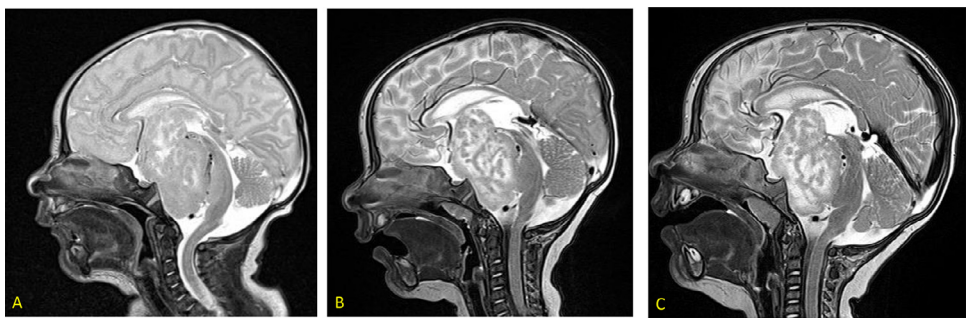

Fig. 4 – Sagittal T2 images through the mass at birth (A), at 3 months (B), and at 5 months (C) of age. Components of the mass are isointense relative to cortex, while others demonstrate T2 hyperintensity. Growth of the mass has been commensurate with the brain.

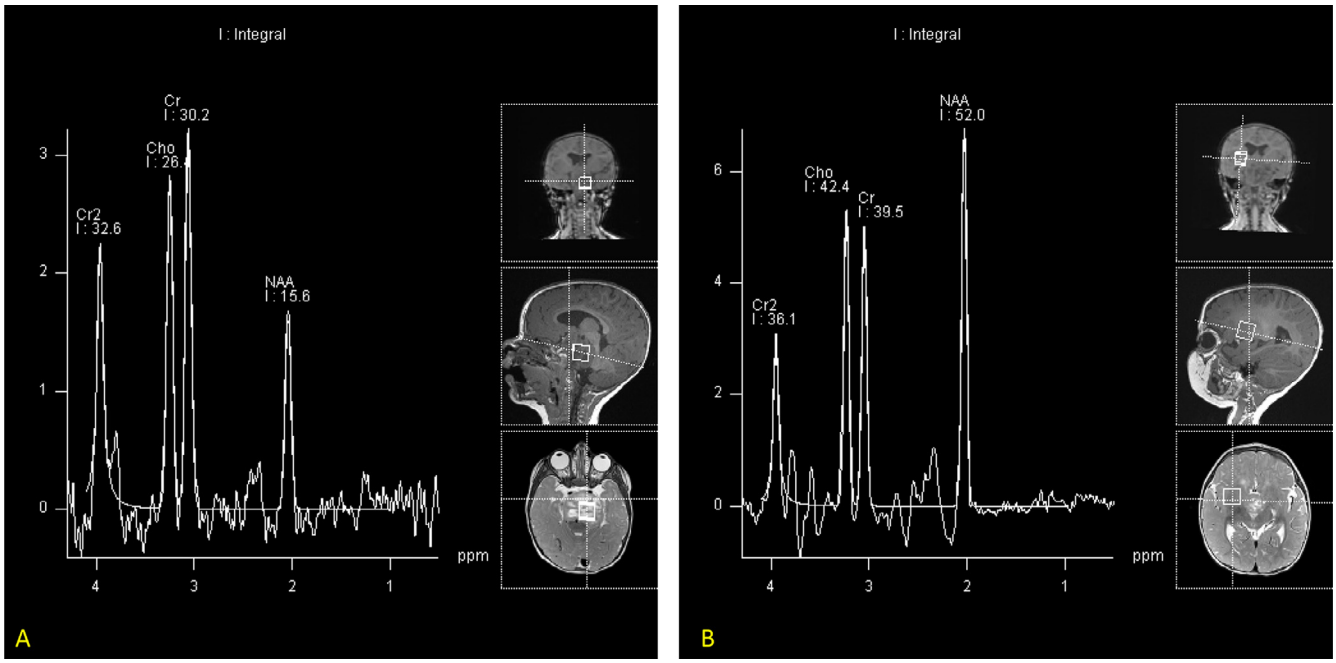

Fig. 5 – Single voxel, intermediate (TE = 135 ms) spectroscopic images performed on a 3T MRI unit at 8 months of life with voxels placed within the lesion (A) and within normal brain parenchyma (B). There is depression of the NAA peak within the lesion. The Cho peak is not elevated within the lesion.

a few reports of these lesions identified and assessed prenatally by fetal MR [5,10,11]. Acharya et al. described a brain "cyst" identified by fetal MR during the ninth month of gestation, with GHH only considered after a postnatal MR demonstrated both solid and cystic components [10]. Booth et al. described an "anterior suprasellar soft tissue lesion with cysts in the suprasellar and prepontine cisterns as well as extension into both middle cranial fossae" identified by fetal MR, without reporting the gestational age of the fetus, with GHH diagnosed by biopsy shortly after delivery [11]. Celedin et al. described "a large suprasellar and prepontine mass" in a 37 week fetus with hexadactyly, with GHH within the context of Pallister-Hall syndrome confirmed by postnatal MR [5]. Our case in unique in that the correct diagnosis of GHH was made by fetal MR, in the absence of other corroborative findings (ie, polydactyly).

It is extremely rare to diagnose these lesions when patients are asymptomatic. Isaka et al. published the only case of asymptomatic GHH in a 42-year-old male who presented with acute mild facial numbness [19]. Fortunately, our patient has demonstrated normal development without detected clinical or laboratory abnormalities but will continue to be followed by our clinical services.

The postnatal course of hamartomas shows proportional growth to that of normal brain tissue [5,16,26]. It has been suggested that hamartomas receive a majority of proliferative stimuli between 25th and 41st day postconception during the normal development of the hypothalamus [16,21]. Prenatal diagnosis supports evidence that these lesions develop prior to 25 weeks gestation, as reported by Booth et al. Additionally, these lesions do not usually grow after identification on imaging [13,17,20]. Although the lesion in our case did progressively increase in size, it did so commensurate with the growth of the brain, and remained stable in size from age 5 to 8 months. Tonami et al. however described a rare case of a HH diagnosed in an infant with a stable MR appearance until 2 years 4 months old. By 3 years 10 months age, the lesion in this patient showed a significant signal intensity change and later developed precocious puberty at age 4 [13]. Because this patient initially had a HH with the classic MR appearance and developed new imaging and clinical findings later in childhood, this indicates that HH can evolve in both morphology and physiologic impact over time.

The mechanism of GHH development is not completely understood though Dorfer et al. postulate 2 hypotheses. The first of which is that HH are the result of ectopic localization of otherwise normal hypothalamic cells. This could possibly be explained by deficits in cell-cell recognition or cell-matrix interference, which normally guide cells during neuronal migration. The second hypothesis suggests that HH cells are positioned normally but have abnormal proliferative potential leading to the abnormal brain structure. Dorfer et al. supported the latter hypothesis given the large, predominately cystic lesion in their case. Our case would also support the latter hypothesis as the lesion showed areas of small suspected cystic changes.

The available literature demonstrates the typical postnatal MRI findings of GHH: a lesion that is homogenously isointense to gray matter on T1-weighted images, which is iso- to slightly hyperintense on T2-weighted images, and which generally demonstrates no enhancement [7,8,11–15,20,21,25,26]. Lack of contrast enhancement reflects an intact blood-brain barrier [7,21]. Freeman et al. reviewed 72 cases of HH which confirmed these MRI findings though many of their cases showed slightly

decreased T1-weighted signal intensity relative to gray matter for which the authors related to the inversion-prepared gradient-echo sequences they used vs the conventional spin-echo imaging used in most other reports [17].

There is a relative paucity of information available in the literature about the appearance of GHH on fetal MRI. While other reports describe only using T2-weighted imaging [5,10,11], at our institution we routinely include a number of different sequences tailored for fetal MR to help us characterize intracranial lesions. This also includes a T1 spoiled gradient echo sequence, echo planar sequences, as well as DWI. The T1 is helpful to exclude subacute blood products, which would be expected to appear hyperintense. Both the echo planar and T1 sequences are useful to exclude calcification (for example in the setting of intracranial teratoma), which on the former would be expected to demonstrate areas of susceptibility artifact. The DWI was particularly helpful in demonstrating that the mass had similar diffusion characteristics relative to the adjacent normal brain. Areas of restricted diffusion within the mass would have been indicative of hypercellularity, and would have indicated other more aggressive etiologies such as embryonal tumor or astrocytoma [18]. To our best knowledge, there has been no previous report of using DWI on fetal MR in the prenatal diagnosis of GHH. There have been few publications regarding MR spectroscopy of HH and GHH though the available literature suggest that these lesions do not have an elevated choline peak [11,14,15] and often show low to normal levels of N-acetylaspartate (NAA) [17,20]. The low levels of NAA seen in these lesions are interpreted as neuronal loss or dysfunction [17,20]. Our case demonstrated spectroscopic findings similar to the published literature.

Other considerations for a patient found to have a GHH include syndromic conditions, most notably Pallister-Hall syndrome, which account for about 10% of all HH cases [7,16]. Patients with Pallister-Hall syndrome can have hypothalamic hamartoma associated with polydactyly, syndactyly, imperforate anus, bifid epiglottis, renal abnormalities, and pulmonary segmentation anomalies [5,26]. Our patient did not show such findings. A downstream effector protein of the sonic hedgehog pathway, Gli3, has been found to be mutated in some patients with HH associated with Pallister-Hall syndrome. This possibly explains the spectrum of associated brain anomalies found in syndromic patients [16].

The major differential diagnosis for GHH includes craniopharyngiomas, optic pathway-hypothalamic gliomas, and germinomas [5,21,26]. Craniopharyngiomas are cystic or predominately cystic masses which regularly contain areas of calcification. In optic pathway-hypothalamic gliomas, MR imaging typically show an infiltrative lesion of the optic pathways and/or hypothalamus with T2 signal hyperintensity and variable degrees of contrast enhancement. Germinomas are generally solid, enhancing masses involving the infundibulum that demonstrate restricted diffusion.

The treatment for HH depends on the severity of symptoms, the size of the mass, and the location of the mass. Asymptomatic patients can be followed clinically. In symptomatic patients and no evidence of mass effect, invasive treatments such as radiofrequency ablation or radiosurgery could be considered [7]. In more symptomatic patients, such as those with central precocious puberty or medically intractable seizures, evidence supports surgical treatment to facilitate complete disconnection, if feasible [10,14,20,27]. It has been shown that patients may still suffer from seizures with only partial resection [23]. In a case series of 16 GHH treated with stereotactic radiofrequency thermocoagulation by Shirozu et al. [23], they suggested better seizure outcomes without permanent complications compared to other surgical methods suggested by older literature.

Conclusion

In cases of suspected fetal intracranial lesions identified by ultrasound, fetal MRI can provide significant additional information in the assessment and characterization of these lesions. Fetal MRI has many advantages over ultrasound including superior soft tissue contrast, noninterference by the calvarium, and the ability to perform multimetric analysis through the utilization of difference sequences tailored to assess specific properties of the lesion. We present an example of how these advantages of MR were used to diagnosis an intrauterine giant hypothalamic hamartoma, and to the best of our knowledge offer the first published report on how DWI in the fetus may be very useful in the diagnosis of this rare entity.

REFERENCES

[1] Raybaud Charles C, Patay Z, Barkovich J. Intracranial, Orbital, and Neck Masses. Pediatric Neuroimaging. Sixth. Philadelphia: Lippincott Williams and Wilkins; 2018. p. 787–8.

[2] Li CD, Luo SQ, Tang J, Jia G, Ma ZY, Zhang YQ. Classification of hypothalamic hamartoma and prognostic factors for surgical outcome. Acta Neurol Scand Jul. 2014;130(1):18–26. doi:10.1111/ane.12209.

[3] Valdueza JM, Cristante L, Dammann O, Bentele K, Vortmeyer A, Saeger W, et al. Hypothalamic hamartomas: with special reference to gelastic epilepsy and surgery. Neurosurgery 1994;34(6):949–58 discussion 958. doi:10.1227/00006123-199406000-00001.

[4] O. Delalande and M. Fohlen, "Disconnecting surgical treatment of hypothalamic hamartoma in children and adults with refractory epilepsy and proposal of a new classification," 2020, doi: https://doi.org/10.2176/nmc.43.61.

[5] Celedin S, Kau T, Gasser J, Kraschl R, Sinzig M. Fetal MRI of a hypothalamic hamartoma in Pallister-Hall syndrome. Pediatric Neurol 2010;42(1):59–60. doi:10.1016/j.pediatrneurol.2009.08.003.

[6] Mittal S, Mittal M, Montes JL, Farmer J-P, Andermann F. Hypothalamic hamartomas. Part 1. Clinical, neuroimaging, and neurophysiological characteristics. Neurosurg Focus 2013;34(6):E6. doi:10.3171/2013.3.FOCUS1355.

[7] Alves C, Barbosa V, Machado M. Giant hypothalamic hamartoma: case report and literature review. Childs Nerv Syst 2013;29(3):513–16. doi:10.1007/s00381-013-2022-y.

[8] Guibaud L, Rode V, Saint-Pierre G, Pracros J-P, Foray P, Tran-Minh VA. Giant hypothalamic hamartoma: an unusual neonatal tumor. Pediatr Radiol 1995;25(1):17–18. doi:10.1007/BF02020833.

[9] Hubbard AM, Egelhoff JC. MR imaging of large hypothalamic hamartomas in two infants. American Journal of Neuroradiology 1989;10(6):1277.

[10] Acharya S, Gopal R, Menon P, Bandgar T, Shah N. A rare case of central precocious puberty due to hypothalamic hamartoma diagnosed in utero. Endocr Pract 2009;16(2):237–40. doi:10.4158/EP09193.CR.
[11] Booth TN, Timmons C, Shapiro K, Rollins NK. Pre- and postnatal MR Imaging of hypothalamic hamartomas associated with arachnoid cysts. Am J Neuroradiol 2004;25(7):1283–5.
[12] Nishio S, Morioka T, Hamada Y, Kuromaru R, Fukui M. Hypothalamic hamartoma associated with an arachnoid cyst. J Clin Neurosci 2001;8(1):46–8. doi:10.1054/jocn.2000.0771.
[13] Tonami H, Higashi K, Okamoto K, Akai T, Iizuka H, Nojima T, et al. Report of changing signal intensity on follow-up MRI in a case of hypothalamic hamartoma. J Comput Assisted Tomograph 2001;25(1):130–2.
[14] Kandregula S, Savardekar AR, Nandeesh BN, Arivazhagan A, Rao MB. Giant hypothalamic hamartoma in an infant: a case report and review of the literature. PNE 2017;52(1):55–61. doi:10.1159/000448738.
[15] Lee JY, Yoon H-K, Khang SK. Giant hypothalamic hamartoma associated with an intracranial cyst in a newborn. Ultrasonography 2016;35(4):353–8. doi:10.14366/usg.15080.
[16] Dorfer C, Kasprian G, Mühlebner A, Czech T. Giant solid-cystic hypothalamic hamartoma: case report. Neurosurg Focus 2011;30(2):E7. doi:10.3171/2011.1.FOCUS10240.
[17] Freeman JL, Coleman LT, Wellard RM, Kean MJ, Rosenfeld JV, Jackson GD, et al. MR imaging and spectroscopic study of epileptogenic hypothalamic hamartomas: analysis of 72 cases. Am J Neuroradiol 2004;25(3):450–62.
[18] Cabet S, Meyronet D, Fichez A, di Rocco F, Gauthier-Moulinier H, Guibaud L. Embryonal tumor of posterior cerebral fossa: false-negative diagnosis by fetal MRI related to misinterpretation of decreased apparent diffusion coefficient. Ultrasound Obstet Gynecol 2019;53(4):551–3. doi:10.1002/uog.19095.
[19] Isaka T, Nakatani S, Yoshimine T, Akai F, Taneda M. Asymptomatic hypothalamic hamartoma associated with an arachnoid cyst —case report. Neurologia Medico-Chirurgica 1996;36(10):725–8. doi:10.2176/nmc.36.725.
[20] Miranda P, Esparza J, Cabrera A, Hinojosa J. Giant hypothalamic hamartoma operated through subfrontal approach with orbitary rim osteotomy. Pediatric Neurosurg 2006;42(4):254–7. doi:10.1159/000092365.
[21] Prasad S, Shah J, Patkar D, Gala B, Patankar T. Giant hypothalamic hamartoma with cystic change: report of two cases and review of the literature. Neuroradiology 2000;42(9):648–50. doi:10.1007/s002340000350.
[22] Razzaq AA, Chishti MK. Giant hypothalamic hamartoma and associated seizure types. J Pak Med Assoc 2001;51(8):296–8.
[23] Shirozu H, Masuda H, Ito Y, Sonoda M, Kameyama S. Stereotactic radiofrequency thermocoagulation for giant hypothalamic hamartoma. J Neurosurg 2016;125(4):812–21. doi:10.3171/2015.6.JNS15200.
[24] Aran E, Pereira J, Vaz R, Castro L. Voluminoso hamartoma hipotalámico en un niño de 5 meses: Epilepsia y cirugía. Neurocirugía 2004;15(3):294–7. doi:10.1016/S1130-1473(04)70487-X.
[25] López-Laso E, González MEM, León RC, González MDJ, Rodríguez JE. Giant hypothalamic hamartoma and dacrystic seizures. Epileptic Disord 2007;9(1):90–3. doi:10.1684/epd.2007.0068.
[26] Kuo JS, Casey SO, Thompson L, Truwit CL. Pallister-Hall syndrome: clinical and MR features. Am J Neuroradiol 1999;20(10):1839–41.
[27] Kerrigan JF, Ng Y, Prenger E, Krishnamoorthy KS, Wang NC, Rekate HL. Hypothalamic hamartoma and infantile spasms. Epilepsia 2007;48(1):89–95. doi:10.1111/j.1528-1167.2006.00835.x.